Values and Impacts of Incorporating Local Flexibility Services in Transmission Expansion Planning

Erik F. Alvarez,
Luis Olmos, and Andres Ramos,
Institute for Research in Technology (IIT)
Comillas Pontifical University
28015 Madrid, Spain
{ealvarezq; luis.olmos; andres.ramos}@comillas.edu

Kyriaki Antoniadou-Plytaria,
David Steen, and Le Anh Tuan
Department of Electrical Engineering
Chalmers University of Technology
41296 Gothenburg, Sweden
{kyriaki.antoniadou; david.steen; tuan.le}@chalmers.se

***Abstract*—This paper presents a cost-based TSO-DSO coordination model to quantify the value of local flexibility services and analyze its impact on the transmission grid expansion and the system operation. Flexibility is provided to the DC power flow transmission grid model by microgrids within the integrated AC power flow distribution grid model. The model's objective is to minimize the overall cost of transmission investments and procured flexibility and is achieved using a bilevel optimization approach where the power exchanges on all connected grid interfaces are controlled. Case studies using a combined test system of the IEEE RTS-96 transmission network interfacing multiple 33-bus distribution grids were performed to validate the model and assess the values and impacts of local flexibility on the transmission system expansion. The results showed that the proposed model modified the investment plan and dispatch of flexibility resources reducing the investment and operation cost of the transmission system.**

***Index Terms*—Distribution and transmission system coordination, flexibility service, microgrids, transmission expansion.**

NOTATION

Sets:

$\mathcal{B}$	Set of transmission network buses.
$\mathcal{C}$	Set of circuits.
$\mathcal{F}_{i'}$	Set of buses with a line connecting them to bus i'.
$\mathcal{G}$	Set of generating units.
$\mathcal{H}$	Set of time discretization steps (simulation horizon).
$\mathcal{H}_f$	Set of time steps belonging to the flexibility activation period.
$\mathcal{K}/\mathcal{P}$	Set of charging/discharging sample data.
$\mathcal{L}$	Set of branches, where $\mathcal{L} \subseteq \mathcal{B} \times \mathcal{B}$.
$\mathcal{M}_{i'}$	Set of buses i' that are common coupling points with a MG.
$\mathcal{N}$	Set of distribution network buses.
$\mathcal{S}_i$	Set of boundary buses (buses with TSO-DSO interfaces).

Indices:

i, j	Transmission network buses.
i', j'	Distribution network buses (within the same distribution grid).
m	Distribution network bus with a connected microgrid.
ijc	Line.
c	Circuit.
g	Generator (thermal, RES, or ESS).
k/p	Index for discharging/charging sample data.
t	Index for time discretization step.

I. INTRODUCTION

The transition to a zero-carbon economy is driving new planning and operational challenges focused on increasing flexibility. Traditionally, the expansion planning of the transmission system contributes to it. Still, it needs new tools in order to represent the current situation better with the purpose of developing technical-economical efficient plans. Moreover, as a result of the increasing deployment of distributed generation and storage units, distributed energy resources (DERs) should also contribute part of this flexibility, which requires the transmission and distribution system operators (TSO & DSO) to coordinate the operation of their grids. But the massive provision of flexibility services (FSs) at the local level, within the distribution network, should potentially be conditioning not only the operation of the system but also the expansion of the transmission grid.

Several TSO-DSO operation coordination models are defined and assessed in the literature, see [1] and [2]. Some previous works (e.g., [2], [3]) consider the provision of local flexibility in the context of the coordination of the operation of the TSO and DSO grids. However, most of these works do not consider the expansion of the system. An exception to this is the work in [4], where the joint planning of the expansion of the transmission and distribution networks is modeled in a trilevel problem aimimg at minimizing the transmission and distribution investment costs while optimizing the operation of the system by computing the economic dispatch. However, the authors do not consider the option of DERs providing flexibility to the system, both at the operation and at the expansion planning levels, according to several possible operation strategies. As far as we know, the assessment of the impact of the provision of local flexibility on the operation and expansion of the transmission system and the associated costs, according to centralized and decentralized operation schemes, has not been explored before.

In this paper, we define optimization models at different levels of network operation to formulated and solve the optimization problems corresponding to the study cases described in Section III, for the coordinated planning of the expansion of the transmission grid, its operation, and the operation of the downstream distribution grids where

microgrids (MGs) operating flexible DERs are connected. Comparing the network expansion and operation results along with their associated costs acquired by the solution of these problems, we determine the impact of local FSs on the transmission expansion planning (TEP) and the operation of the system, as well as the economic value that FSs offer to the system. Our models consider the detailed representation of the transmission & distribution networks, including the MGs connected to the latter, where DERs are located. We model the transmission network expansion computation and the system operation at transmission and distribution level as a mixed-integer programming (MIP) problem, considering the DC power flow model at transmission level and the AC branch flow model at distribution level. Combining these models results in a multilevel optimization problem which is computationally challenging to solve and, usually, tractable only for small test systems. Similar to the authors in [4], we transform our multilevel problem into an equivalent single-level problem. In addition, we represent the detailed operation of the MGs according to a multi-follower approach and consider the power exchanges among the transmission grid, the distribution grid, and the MGs as the variables for the coordination of the several problems addressed. The main research questions addressed in our work are as follows:

1) How does the choice of the model considered for the TSO-DSO coordination affect the operation of the system and, specifically, the dispatch of local flexibility resources (DERs providing flexibility)?
2) How does this choice of coordination model affect the amount, allocation, and value of the local FSs?
3) How does the provision of local FSs affect the expansion of the transmission grid?

The main contributions of the paper are described next:

- An optimization model to solve the TEP considering TSO-DSO coordination and utilization of locally provided FSs. The local flexibility can be procured centrally by the TSO or in a decentralized manner i.e., by each DSO. The model is used to assess the flexibility value of the system and determine its impact on the expansion of the transmission network and the operation of the system.
- A detailed representation of the provision of local flexibility considering two FSs: 1) a baseline product that quantifies flexibility as the deviation from a power profile and is typically used in recent studies, and 2) a capacity limitation product that quantifies flexibility as the peak power reduction from an upper capacity limit and was introduced in [5] to avoid possible market manipulation. The comparison of the transmission system expansion and operation results considering these FSs offered at different system levels allows us to determine which approach provides higher benefits to the TSO.
- A bilevel optimization problem formulated using: 1) a multi-follower approach for the MGs connected at the distribution level and 2) the optimization model's variables representing the power exchanges among grids as the means to coordinate optimization problems at different network levels. Then, transforming the resulting bilevel problem into an equivalent single-level one, we manage to solve it in an easily scalable way for any system, unlike previous works addressing this type of problem.

II. Model Formulation

Our TSO-DSO model comprises three main parts: a) the TEP and operation problem solved by the TSO; b) the operation problem faced by the DSO; and c) the energy and flexibility dispatch problem addressed by each MG offering energy services to its customers and FSs to the grids connected upstream. Each of these problems can be solved separately, computing the power exchange with the neighboring upstream grid and setting the exchanges with the neighboring downstream grids as input parameters. To represent the coordinated operation of the DSO grid and the MGs, we define a bilevel optimization problem following the developing research trend of utilizing bilevel programming to model interactions between resource aggregators (or MGs) and prosumers [6], [7], as well as interactions between grid or market operators and aggregators, MGs or prosumers [8], [9]. The bilevel problem is transformed into an equivalent single-level MIP problem by replacing the lower-level (LL) problem with its Karush–Kuhn–Tucker (KKT) conditions and using the strong duality theorem [10]. The TSO & DSO grid operation coordination is modeled by integrating the aforementioned single-level optimization problem to the TEP problem. This is achieved by combining the objective functions (OFs) of both problems into a single OF and treating the power flows through the transformers at the boundary buses between the transmission and distribution networks as common variables.

This section separately provides the formulation of each part of our global model. The problem formulation corresponding to each test case, representing a specific coordination paradigm, is provided in Section III.

A. TEP Problem: Constraints

The formulation proposed for the transmission planning problem is based on that in the existing open-source model *openTEPES* by [11], where network investment decisions are computed for future years considering hourly resolution in the future system operation. Candidate lines are pre-defined by the user, so the model determines the optimal investment decisions among those specified as options using a DC-OPF linearized approximation. The formulation of the TEP problem solved by the TSO is given by (1) s.t. (2)–(10).

1) OF: The TSO aims at minimizing, in (1), the total investment costs (first term) and the total operation cost related to the generation dispatch and load shedding (last two terms):

$$\min \sum_{ijc \in \mathcal{L}^c} C^{line}_{ijc} ict_{ijc} + \sum_{tg} \Delta t CV_g p_{tg} + \sum_{ti} \Delta t C^{ens} l^{shed}_{ti}. \quad (1)$$

The parameters $C^{line}_{ijc}, CV_g, C^{ens}$ represent the annualized fixed cost of a candidate line, the variable generation cost, and the cost of unserved energy, respectively. Variable cost includes fuel, operation and maintanance (O&M) and emission

cost. Moreover, Δt is the duration of the time discretization step. The variables l_{ti}^{shed}, p_{tg}, and the (relaxed) binary variable ict_{ijc} denote the load shedding, the active power generation, and the decision on candidate line installation, respectively.

2) Power Balance: The balance of generation and demand at each node disregarding ohmic losses is given by

$$\sum_{g\in\mathcal{G}_i} p_{tg} - P_{ti}^{d} - \sum_{i'\in\mathcal{S}_i} p_{ti'}^{SS} - l_{ti}^{shed} - \sum_{ijc\in\mathcal{L}} f_{tijc}^{P} + \sum_{jic\in\mathcal{L}} f_{tjic}^{P} = 0,\ \forall t\in\mathcal{H},\ \forall i\in\mathcal{B}, \tag{2}$$

where parameter P_{ti}^{d} is the active power demand, and variables f_{tijc}^{P}, $p_{t,i'}^{SS}$ refer to the active power flow on the lines and the active power transferred to the connected distribution grids through the border substations, respectively.

3) Logical Investment Bounds: The transfer capacity in candidate transmission lines is given by

$$-ict_{ijc} \le \frac{f_{tijc}^{P}}{\overline{S}_{ijc}} \le ict_{ijc} \qquad \forall tijc, ijc\in\mathcal{L}^{c} \tag{3}$$

where $\overline{S}_{ijc}$ is the line's total transfer capacity multiplied by a security coefficient (e.g., 0.67 was taken in our approach).

4) Power Flow Bounds: The DC power flow for existing and candidate lines (Kirchhoff's second law) is given by

$$\frac{f_{tijc}^{P}}{\overline{S}_{ijc}^{'}} = (\theta_{ti} - \theta_{tj})\, B_{ijc} \frac{S_B}{\overline{S}_{ijc}^{'}} \qquad \forall tijc, ijc\in\mathcal{L}^{e} \tag{4}$$

$$\left|\frac{f_{tijc}^{P}}{\overline{S}_{ijc}^{'}} - (\theta_{ti}-\theta_{tj}) B_{ijc} \frac{S_B}{\overline{S}_{ijc}^{'}}\right| \le 1 - ict_{ijc} \qquad \forall tijc, ijc\in\mathcal{L}^{c} \tag{5}$$

Where θ_{ti} and B_{ijc} are the bus voltage angle and the susceptance of each line in p.u., respectively. $\overline{S}_{ijc}^{'}$ is the big M of the disjunctive constraint.

5) Transmission System Bounds: The bounds on generation, load shedding, and network transfer capacity are defined by Eqs. (6)-(8), while the decision variables for line installation are limited by (9):

$$\underline{P}_g \le p_{tg} \le \overline{P}_g \qquad \forall t\in\mathcal{H}, \forall g\in\mathcal{G}, \tag{6}$$

$$0 \le l_{ti}^{shed} \le P_{ti}^{d} \qquad \forall t\in\mathcal{H},\ \forall i\in\mathcal{B}, \tag{7}$$

$$-\overline{S}_{ijc} \le f_{tijc}^{P} \le \overline{S}_{ijc} \qquad \forall tijc, ijc\in\mathcal{L}^{e}, \tag{8}$$

$$ict_{ijc} \in \{0,1\} \qquad \forall ijc, ijc\in\mathcal{L}^{c}. \tag{9}$$

$\underline{P}_g$ and $\overline{P}_g$ are the minimum load and maximum capacity of each generator and $\overline{S}_{ijc}$ is the maximum line capacity.

The voltage angle of the reference node is set to 0 for each time step according to the constraint (10):

$$\theta_{t,node_{ref}} = 0 \qquad \forall t\in\mathcal{H}. \tag{10}$$

B. DSO: Optimal Network Operation Problem (Upper Level)

In this paper, the DSO optimizes its operation using the FS offered by the grid-connected MGs, who are the flexible service providers (FSPs). The two FSs considered are illustrated in Fig. 1 and represented in Section II-B3 as FS-C, for the flexibility offered as a capacity limitation product; and FS-B, for the flexibility offered as a baseline product.

1) OF: The DSO's objective is to minimize its peak power cost and the cost of the provisioning of local flexibility, which leads to the minimization of the subscription fee paid to the TSO. The OF is given by

$$\min f^{UL,peak} = c^{peak} + c^{flex}, \tag{11}$$

where c^{peak} is the peak power cost and c^{flex} is the cost of purchasing local flexibility from the MGs.

2) Power Flow Equations: The LinDistFlow equations (13)–(21) $\forall t \in \mathcal{H}$ model the linearized lossless AC power flow according to the convex branch flow model [12], which is derived after applying voltage angle relaxation and disregarding the capacitance and the line losses. Eq. (12) $\forall t \in \mathcal{H}$ is added for the calculation of c^{peak}.

$$c^{peak} \ge \Lambda^{peak} p_{ti'}^{SS} \qquad \forall t\in\mathcal{H}, \forall i'\in\mathcal{N}\cup\mathcal{S}_i, \tag{12}$$

$$-\sum_{m\in\mathcal{M}_{i'}} (p_{tm}^{MG,im} - p_{tm}^{MG,ex}) - P_{ti'}^{L} + \sum_{i'\in\mathcal{S}_i} p_{ti'}^{SS} + \sum_{j'\in\mathcal{F}_{i'}} (p_{tj'i'} - p_{ti'j'}) = 0, \quad \forall t\in\mathcal{H}, \forall i', j'\in\mathcal{N}, \tag{13}$$

$$-q_{ti'}^{SS} - Q_{ti'}^{L} - \sum_{m\in\mathcal{M}_{i'}} Q_{tm}^{MG} + \sum_{j\in\mathcal{F}_{i'}} (q_{tj'i'} - q_{ti'j'}) = 0, \quad \forall t\in\mathcal{H}, \forall i', j'\in\mathcal{N}, \tag{14}$$

$$v_{tj'} - v_{ti'} + 2(p_{ti'j'} R_{i'j'} + q_{ti'j'} X_{i'j'}) = 0, \quad \forall t\in\mathcal{H}, \forall i'\in\mathcal{N}, \forall j'\in\mathcal{F}_{i'}, \tag{15}$$

$$v_{ti'} \le V^{max} \quad \text{and} \quad v_{ti'} \ge V^{min}, \qquad \forall t\in\mathcal{H}, \forall i'\in\mathcal{N}, \tag{16}$$

$$v_{ti'} = V^{SB}, \qquad \forall t\in\mathcal{H}, \forall i'\in\mathcal{S}_i, \tag{17}$$

$$p_{ti'j'} = 0, \qquad \forall t\in\mathcal{H}, \forall i'\in\mathcal{N}, \forall j'\notin\mathcal{F}_{i'}, \tag{18}$$

$$q_{ti'j'} = 0, \qquad \forall t\in\mathcal{H}, \forall i'\in\mathcal{N}, \forall j'\notin\mathcal{F}_{i'}, \tag{19}$$

$$p_{ti'j'} + p_{tj'i'} = 0, \qquad \forall t\in\mathcal{H}, \forall i'\in\mathcal{N}, \forall j'\notin\mathcal{F}_{i'}, \tag{20}$$

$$q_{ti'j'} + q_{tj'i'} = 0, \qquad \forall t\in\mathcal{H}, \forall i'\in\mathcal{N}, \forall j'\notin\mathcal{F}_{i'}, \tag{21}$$

The variables $p_{tm}^{MG,ex}$/$p_{tm}^{MG,im}$ denote the power exported from, or imported into an MG. The variables $v_{ti'}$ and $p_{ti'j'}$/$q_{ti'j'}$ refer to square of voltage magnitude and active/reactive power flows. The parameters Λ^{peak}, $R_{i'j'}$/$X_{i'j'}$, and V^{SB} refer to peak imported power tariff paid by the DSO to the TSO, line resistance/reactance, and square of voltage at the distribution grid's substation (boundary bus). And, the parameters $P_{ti'}^{L}, Q_{ti'}^{L}$ refers to the active and reactive power demand at distribution nodes, respectively.

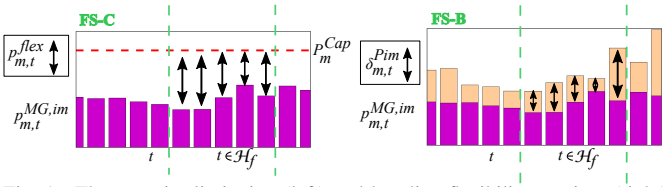

Fig. 1. The capacity limitation (left) and baseline flexibility services (right).

3) FSs: This section refers to the next FSs: FS-C and FS-B. **FS-C:** Regarding the flexibility product FS-C, the term c^{flex} of (11) becomes

$$c^{flex} = \sum_{t\in\mathcal{H}_f}\sum_{t\in\mathcal{M}_{i'}} \pi^{Cap}_{flex} p^{flex}_{tm} = \pi^{Cap}_{flex}(P^{Cap}_m - p^{fl,im}_{tm}) \quad (22)$$

and the MG imported/exported power are given by

$$p^{MG,im}_{tm} = p^{im}_{tm}, \qquad \forall t \in \mathcal{H},\ \forall m \in \mathcal{M}_{i'}, \quad (23)$$

$$p^{MG,ex}_{m,t} = p^{ex}_{m,t}, \qquad : \ \forall t \in \mathcal{H},\ \forall m \in \mathcal{M}_{i'}, \quad (24)$$

The positive variables π^{Cap}_{flex} and p^{flex}_{tm} are the flexibility price and the offered amount of flexibility (average value over Δt) during the flexibility activation period $\mathcal{H}_f \subseteq \mathcal{H}$. And, $p^{fl,im}_{tm}$ is the MG's imported power at each time step of the flexibility activation period. Note that the amount of flexibility is calculated in terms of power capacity reduction, i.e., the mobilization of the flexibility product FS-C results in an "updated" capacity given by $P^{Cap}_m - p^{flex}_{m,t}$ to the DSO. The parameter P^{Cap}_m is the upper capacity limit, and it should be based on a value that the DSO and the MG operator can easily agree upon, such as, e.g., the capacity at the connection point. **FS-B:** Regarding the flexibility product FS-B, the term c^{flex} of (11) becomes

$$c^{flex} = \sum_{t\in\mathcal{H}_f}\sum_{m\in\mathcal{M}_{i'}} -\pi^{im}_{flex}\delta^{Pim} + \pi^{ex}_{flex}\delta^{Pex}, \quad (25)$$

and the MG imported/exported power are given by

$$p^{MG,im}_{tm} = p^{im}_{tm} + \delta^{Pim}, \qquad : \ \forall t \in \mathcal{H},\ \forall m \in \mathcal{M}_{i'}, \quad (26)$$

$$p^{MG,ex}_{m,t} = p^{ex}_{m,t} + \delta^{Pex}, \qquad : \ \forall t \in \mathcal{H},\ \forall m \in \mathcal{M}_{i'}, \quad (27)$$

where the positive variables $\pi^{im}_{flex}, \pi^{ex}_{flex}$ are the flexibility prices and the variables $\delta^{Pim}/\delta^{Pex}$ are the procured flexibility amounts. In this FS, the amount of flexibility provided δ^{Pim} or δ^{Pex} is the deviation from the baseline power exchange profile. In this paper, it is assumed that the baseline profile corresponds to the optimal MG energy dispatch ($p^{ex}_{m,t} - p^{im}_{m,t}$) computed as the solution of the optimal MG energy management problem when no FS is considered.

C. Energy and Flexibility Dispatch of the MGs (LL)

The formulation of the primal LL problem differs if we consider FS-C: given by (28) s.t. (29)–(52), $\forall m \in \mathcal{M}_{i'}$; or if we consider FS-B: given by (28) s.t. (29)–(49) and (53)–(59), $\forall m \in \mathcal{M}_{i'}$. Notice that the dual variables denoted by λ or μ are defined for each constraint and, due to space limitations, inequality constraints are described together with their complementarity slackness (CS) conditions. Though the latter is not part of the primal problem, they will be later used to derive the KKT conditions (see Section II-D).

1) OF: The MG operator seeks to minimize the energy cost of the MG (given by $c^{im}_m - r^{ex}_m$ in (28), where c^{im}_m and r^{ex}_m refer to the energy cost and revenue of the MG.), while maximizing the income from the FSs provided, denoted by r^{flex}:

$$\min f^{LL}_m = c^{im}_m - r^{ex}_m - r^{flex}, \quad (28)$$

$$c^{im}_m = \sum_{t\in\mathcal{H}} (\Lambda_t + C^{im}) p^{MG,im}_{tm} \Delta t, \quad (29)$$

$$r^{ex}_m = \sum_{t\in\mathcal{H}} (\Lambda_t + C^{ex}) p^{MG,ex}_{tm} \Delta t, \quad (30)$$

where the parameter Λ_t is the energy price [€/MWh], while C^{im}, C^{ex} denote the distribution grid tariff and reimbursement fee corresponding to the MG imported and exported energy.

2) Power Balance: An MG connected at bus m with PV and BES systems must satisfy (31) $\forall t \in \mathcal{H}$, since the electricity consumption of the MG customers is supplied through the MG resources and/or the connection with the upstream distribution grid at each time step:

$$P^{PV}_{tm} + p^{dis}_{tm} - p^{ch}_{tm} = p^{MG,ex}_{tm} - p^{MG,im}_{tm} + P^{MG,L}_{tm} : \lambda^{PB}_{tm}. \quad (31)$$

In (31), P^{PV}_{tm}, P^{MGL}_{tm}, and the positive variables p^{ch}_{tm}/p^{dis}_{tm} respectively refer to the PV generation of the MG's PV systems, the electric power consumption of the MG customers, and the charging/discharging power of the MG's BES. It is assumed that the BES draws power from both the main distribution grid and the PVs and injects power into both the main grid and the MG's consumption points.

3) BES Model: The BES model is given by (32)–(49) $\forall t \in \mathcal{H},\ \forall m \in \mathcal{M}_{i'}$. This is a measurement-based model, which was first presented in [13], that uses a sampling-based approach considering data from charging/discharging curves. The parameters $SoE^{ch}_{mk}, P^{+}_{mk}, P^{ch}_{mk}, SoE^{dis}_{mp}, P^{-}_{mp}, P^{dis}_{mp}$ take the values of the sample data. The positive variables p^{-}_t/p^{+}_t represent the power output/input from/into the BES cells, respectively, before/after BES losses are taken into account. E^{max} is the installed BES capacity and soe_{tm} is the state-of-energy (SoE), or charge level, which must lie between the lower and upper limit (SoE^{min} and SoE^{max}, respectively). Eq. (36) sets the BESs's soe_{tm} at the end of the dispatch period (soe^{end}_m) to be equal to its value at the beginning (SoE^{init}_m). The continuous variables x_{tmp} and y_{tmk}, which are associated respectively with the choice of discharging or charging sample data, are used to create convex combinations of soe_{tm}, p^{+}_{tm}, p^{ch}_{tm}. This model also considers the variable charging/discharging efficiencies of the BES system, which are associated with both internal BES losses and DC/DC converter losses, that affect the p^{ch}_{tm}/p^{dis}_{tm} and soe_{tm}. The charging/discharging efficiencies are defined as $\eta^{ch}_{tm} = p^{+}_{tm}/p^{ch}_{tm}$ and $\eta^{dis}_{tm} = p^{dis}_{tm}/p^{-}_{tm}$, respectively, $\forall t \in \mathcal{H}, \forall m \in \mathcal{M}_{i'}$ [13].

$$soe_{tm} = \begin{cases} soe_{tm} = SoE^{init}_m, & : \lambda^{start}_{tm}, t = 1 \\ soe_{t-1,m} + \frac{p^{+}_{t-1,m}\Delta t}{E^{max}_m} - \frac{p^{-}_{t-1,m}\Delta t}{E^{max}_m}, & : \lambda^{BES}_{tm}, t > 1 \end{cases} \quad (32)$$

$$soe^{end}_m = soe_{tm} + \frac{p^{+}_{tm}\Delta t}{E^{max}_m} - \frac{p^{-}_{tm}\Delta t}{E^{max}_m}, \qquad : \lambda^{BES,end}_{tm} \quad (33)$$

$$0 \geq SoE_m^{min} - soe_{tm} \quad \text{to be consistent} \quad \underline{\mu}_{tm}^{SoE} \geq 0, \tag{34}$$

$$0 \geq soe_{tm} - SoE_m^{max} \quad \text{to be consistent} \quad \overline{\mu}_{tm}^{SoE} \geq 0, \tag{35}$$

$$soe_m^{end} = SoE_m^{init}, \qquad : \lambda_{tm}^{end} \tag{36}$$

$$p_{tm}^{-} = \sum_{p \in \mathcal{P}} P_{mp}^{-} x_{tmp}, \qquad : \lambda_{tm}^{-} \tag{37}$$

$$p_{tm}^{dis} = \sum_{p \in \mathcal{P}} P_{mp}^{dis} x_{tmp}, \qquad : \lambda_{tm}^{dis} \tag{38}$$

$$p_{tm}^{+} = \sum_{k \in \mathcal{K}} P_{mk}^{+} y_{tmk}, \qquad : \lambda_{tm}^{+} \tag{39}$$

$$p_{tm}^{ch} = \sum_{k \in \mathcal{K}} P_{mk}^{ch} y_{tmk}, \qquad : \lambda_{tm}^{ch} \tag{40}$$

$$0 \geq -p_{tm}^{ch} \quad \text{to be consistent} \quad \mu_{tm}^{ch} \geq 0, \tag{41}$$

$$0 \geq -p_{tm}^{dis} \quad \text{to be consistent} \quad \mu_{tm}^{dis} \geq 0, \tag{42}$$

$$0 \geq -p_{tm}^{+} \quad \text{to be consistent} \quad \mu_{tm}^{+} \geq 0, \tag{43}$$

$$0 \geq -p_{tm}^{-} \quad \text{to be consistent} \quad \mu_{tm}^{-} \geq 0, \tag{44}$$

$$soe_{tm} = \sum_{p \in \mathcal{P}} SoE_{mp}^{dis} x_{tmp} + \sum_{k \in \mathcal{K}} SoE_{mk}^{ch} y_{tmk} \quad : \lambda_{tm}^{SoE}, \tag{45}$$

$$\sum_{p \in P} x_{tmp} = 1, \qquad : \lambda_{tm}^{x}, \tag{46}$$

$$0 \geq -x_{tmp} \quad \text{to be consistent} \quad \mu_{tmp}^{x} \geq 0, \qquad \forall p \in \mathcal{P}, \tag{47}$$

$$\sum_{k \in K} y_{tmk} = 1, \qquad : \lambda_{tm}^{y}, \tag{48}$$

$$0 \geq -y_{tmk} \quad \text{to be consistent} \quad \mu_{tmk}^{y} \geq 0, \qquad \forall k \in \mathcal{K}, \tag{49}$$

4) Flexibility as a Capacity Limitation Product: The term r^{flex} in (28) becomes

$$r_m^{flex} = \sum_{t \in \mathcal{H}_f} \pi_{flex}^{Cap} (P_m^{Cap} - p_{tm}^{fl,im}) \tag{50}$$

and the following constraints are added $\forall t \in \mathcal{H}, \forall m \in \mathcal{M}_{i'}$:

$$0 \geq p_{tm}^{im} - p_{tm}^{fl,im} \qquad \text{to be consistent} \quad \mu_{tm}^{fl,Cap} \geq 0, \tag{51}$$

$$0 \geq -p_{tm}^{fl,im} \qquad \text{to be consistent} \quad \mu_{tm}^{fl,+} \geq 0, \tag{52}$$

5) Flexibility as a Baseline Product: The MG imported/exported power are given by (26)–(27) while the following constraints are also added $\forall t \in \mathcal{H}, \forall m \in \mathcal{M}_{i'}$:

$$0 \geq -p_{tm}^{im} \qquad \text{to be consistent} \quad \mu_{tm}^{im,+} \geq 0, \tag{53}$$

$$0 \geq -p_{tm}^{ex} \qquad \text{to be consistent} \quad \mu_{tm}^{ex,+} \geq 0, \tag{54}$$

$$0 \geq \delta_{tm}^{Pim} \qquad \text{to be consistent} \quad \mu_{tm}^{fl,im+} \geq 0, \tag{55}$$

$$0 \geq -\delta_{tm}^{Pex} \qquad \text{to be consistent} \quad \mu_{tm}^{fl,ex+} \geq 0, \tag{56}$$

$$0 \geq -p_{tm}^{im} - \delta_{tm}^{Pim} \qquad \text{to be consistent} \quad \mu_{tm}^{fl,im} \geq 0, \tag{57}$$

$$0 \geq -p_{tm}^{ex} - \delta_{tm}^{Pex} \qquad \text{to be consistent} \quad \mu_{tm}^{fl,ex} \geq 0, \tag{58}$$

The term r_m^{flex} in (28) becomes

$$r_m^{flex} = \sum_{t \in \mathcal{H}_f} \pi_{flex}^{ex} \delta_{tm}^{Pex} + \pi_{flex}^{im} \delta_{tm}^{Pim}. \tag{59}$$

D. Bilevel Optimization: DSO and MGs

The formulation of the bilevel problem as a single-level equivalent problem is carried out by adding the KKT conditions of the LL problem to the DSO's upper level problem. The KKT conditions comprise all the equality and inequality conditions of the LL problem (along with the CS conditions of the LL inequalities), which were presented in Sections II-C, and the equality constraints derived from the partial derivatives of the LL Lagrangian function w.r.t. LL primal variables (the derivatives must be equal to zero) , which are represented by equations (60)-(78), $\forall m \in \mathcal{M}_{i'}$, where T is the last time step of the dispatch period. Note that all the primal and dual variables of the LL problem become primal variables of the single-level equivalent problem.

$$\frac{\partial \mathcal{L}}{\partial p_{tm}^{ch}} = 0 = -\lambda_{tm}^{PB} + \lambda_{tm}^{ch} - \mu_{tm}^{ch}, \ \forall t \in \mathcal{H}, \tag{60}$$

$$\frac{\partial \mathcal{L}}{\partial p_{tm}^{dis}} = 0 = \lambda_{tm}^{PB} + \lambda_{tm}^{dis} - \mu_{tm}^{dis}, \ \forall t \in \mathcal{H}, \tag{61}$$

$$\frac{\partial \mathcal{L}}{\partial x_{tmp}} = 0 = -P_{mp}^{-} \lambda_{mt}^{-} - P_{mp}^{dis} \lambda_{tm}^{dis} - SoE_{mp}^{dis} \lambda_{tm}^{SoE} - \lambda_{tm}^{x} - \mu_{tmp}^{x}, \ \forall t \in \mathcal{H}, \ \forall p \in \mathcal{P}, \tag{62}$$

$$\frac{\partial \mathcal{L}}{\partial y_{tmk}} = 0 = -P_m^{+} \lambda_{tm}^{+} - P_{mp}^{ch} \lambda_{tm}^{ch} - SoE_{mk}^{ch} \lambda_{tm}^{SoE} - \lambda_{tm}^{y} - \mu_{tmk}^{y}, \ \forall t \in \mathcal{H}, \ \forall k \in \mathcal{K}, \tag{63}$$

$$\frac{\partial \mathcal{L}}{\partial soe_{tm}} = 0 = -\lambda_{tm}^{BES} + \lambda_m^{start} + \lambda_{tm}^{SoE} + \overline{\mu}_{tm}^{SoE} - \underline{\mu}_{tm}^{SoE}, \ t = 1, \tag{64}$$

$$\frac{\partial \mathcal{L}}{\partial soe_{tm}} = 0 = \lambda_{t,m}^{BES} - \lambda_{t+1,m}^{BES} + \lambda_{tm}^{SoE} + \overline{\mu}_{tm}^{SoE} - \underline{\mu}_{tm}^{SoE}, \ \forall t \in \mathcal{H} \setminus \{1, T\}, \tag{65}$$

$$\frac{\partial \mathcal{L}}{\partial soe_{tm}} = 0 = \lambda_{tm}^{BES} - \lambda_m^{BES,end} + \lambda_{tm}^{SoE} + \overline{\mu}_{tm}^{SoE} - \underline{\mu}_{tm}^{SoE}, \ t = T \tag{66}$$

$$\frac{\partial \mathcal{L}}{\partial p_{tm}^{im}} = 0 = (\Lambda_t + C^{im}) \Delta t + \lambda_{tm}^{PB} + \mu_{tm}^{im,+} - \mu_{tm}^{fl,im}, \ \forall t \in \mathcal{H}_f, \tag{67}$$

$$\frac{\partial \mathcal{L}}{\partial p_{tm}^{ex}} = 0 = -(\Lambda_t + C^{ex}) \Delta t - \lambda_{tm}^{PB} + \mu_{tm}^{ex,+} - \mu_{tm}^{fl,ex}, \ \forall t \in \mathcal{H}_f, \tag{68}$$

$$\frac{\partial \mathcal{L}}{\partial p_{tm}^{+}} = 0 = -\frac{\Delta t}{E_m^{max}} \lambda_{t+1,m}^{BES} + \lambda_{tm}^{+} - \mu_{tm}^{+}, \ \forall t \in \mathcal{H} \setminus \{T\}, \tag{69}$$

$$\frac{\partial \mathcal{L}}{\partial p_{tm}^{+}} = 0 = -\frac{\Delta t}{E_m^{max}} \lambda_{t,m}^{BES,end} + \lambda_{tm}^{+} - \mu_{tm}^{+}, \ t = T, \tag{70}$$

$$\frac{\partial \mathcal{L}}{\partial p_{tm}^{-}} = 0 = -\frac{\Delta t}{E_m^{max}} \lambda_{t+1,m}^{BES} + \lambda_{tm}^{-} - \mu_{tm}^{-}, \ \forall t \in \mathcal{H} \setminus \{T\}, \tag{71}$$

$$\frac{\partial \mathcal{L}}{\partial p_{tm}^{-}} = 0 = -\frac{\Delta t}{E_m^{max}} \lambda_{t,m}^{BES,end} + \lambda_{tm}^{-} - \mu_{tm}^{-}, \ t = T, \tag{72}$$

$$\frac{\partial \mathcal{L}}{\partial \delta_{tm}^{Pim}} = 0 = (\Lambda_t + C^{im})\Delta t + \pi_{flex}^{im} + \lambda_{tm}^{PB} + \mu_{tm}^{fl,im+} - \mu_{tm}^{fl,im}, \ \forall t \in \mathcal{H}_f, \tag{73}$$

$$\frac{\partial \mathcal{L}}{\partial \delta_{tm}^{Pim}} = 0 = (\Lambda_t + C^{im})\Delta t + \lambda_{tm}^{PB} + \mu_{tm}^{fl,im+} - \mu_{tm}^{fl,im}, \ \forall t \in \mathcal{H} \cap \mathcal{H}'_f, \tag{74}$$

$$\frac{\partial \mathcal{L}}{\partial \delta_{tm}^{Pex}} = 0 = -(\Lambda_t + C^{ex})\Delta t - \pi_{flex}^{ex} - \lambda_{tm}^{PB} - \mu_{tm}^{fl,ex+} - \mu_{tm}^{fl,ex}, \ \forall t \in \mathcal{H}_f, \tag{75}$$

$$\frac{\partial \mathcal{L}}{\partial \delta_{tm}^{Pex}} = 0 = -(\Lambda_t + C^{ex})\Delta t - \lambda_{tm}^{PB} - \mu_{tm}^{fl,ex+} - \mu_{tm}^{fl,ex}, \ \forall t \in \mathcal{H} \cap \mathcal{H}'_f, \tag{76}$$

$$\frac{\partial \mathcal{L}}{\partial p_{tm}^{fl,im}} = 0 = \pi_{flex}^{Cap} - \mu_{tm}^{fl,+} - \mu_{tm}^{fl,Cap}, \ \forall t \in \mathcal{H}_f, \tag{77}$$

$$\frac{\partial \mathcal{L}}{\partial p_{tm}^{fl,im}} = 0 = -\mu_{tm}^{fl,+} - \mu_{tm}^{fl,Cap}, \ \forall t \in \mathcal{H} \cap \mathcal{H}'_f, \tag{78}$$

III. Test Cases, Assumptions, and Parameters

This section presents the test system and the study cases, as well as the assumptions which were used in the simulations that validated the performance of the proposed model. All the formulated optimization problems were solved using Gurobi 9.1.2 as a commercial MIP solver on a computer with a 3.40 GHz Intel Core i7-10875H processor and 32 GB of RAM. Moreover, the simulations were set up in Python 3.9.4, where Pyomo 6.0.1 was used to develop the optimization models.

A. Test System

The performance of the proposed model is validated on a case study featuring the modified single area IEEE RTS-96 system [14], as its transmission network, and a standard 33-bus radial distribution network [15] representing each connected distribution system. Our model could also be applied to a Case Study featuring real transmission [16] or distribution [17] grids. However, this has been left for future work. Note that it is common practice in studies modeling both transmission and distribution networks to use test systems at least for one network level e.g., [18]. A real-world case study would need detailed data of a real transmission grid and all its downstream connected networks. These data are rarely available.

Three grid-connected MGs are considered on the distribution network at the buses shown in Fig. 2, while their locations in the transmission network are given in Fig. 3. The MGs at distribution nodes 13, 18, and 30 have a BES energy-to-power ratio of 17.2kWh/14.4kW, 25.9kWh/21.6kW, and 134.9kWh/111.76kW, respectively. The complete data can also be found online in a folder named "TSO-DSO coordination"[1] in the repository of the openTEPES model[11]. At each transmission node where there is a connection point for a distribution grid, 10 of the aforementioned standard distribution networks were assumed to be connected. Therefore, in total, 80 distribution networks and 240 grid-connected MGs were considered system-wide. The total projected system load is 6783.37 MW, 10% of which is distributed between the distribution networks and grid-connected MGs. Note that the system load and the power generation capacity were 2.38 times higher than the original data in order to use the test system for transmission expansion planning purposes. The existing transmission grid comprises 33 lines and 5 power transformers; candidate network investments include the duplication of all the network lines and transformers, and their cost is system-dependent. The flexibility activation period considered is 16:00-20:00, which lies within the activation periods requested from small to medium-sized companies offering flexibility in [19].

[1] https://github.com/IIT-EnergySystemModels/openTEPES/tree/master/cases/TSO-DSO_coordination/RTS24a

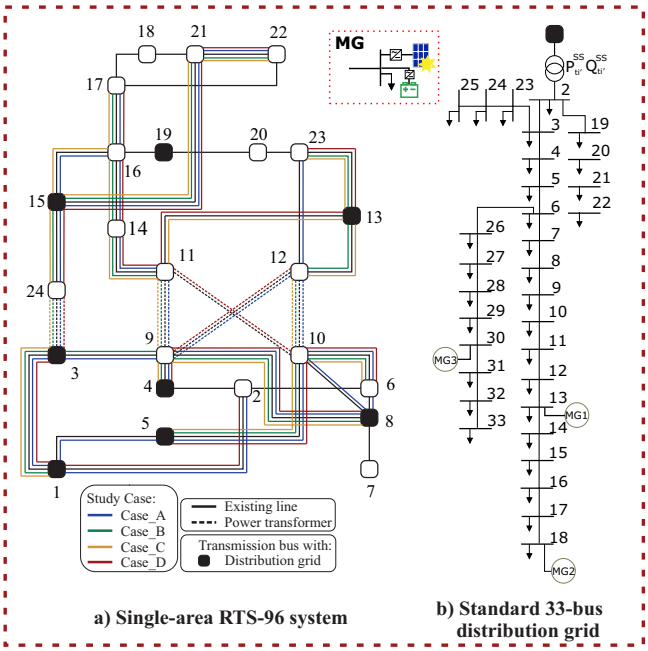

Fig. 2. Representation of the network topology with single-line diagrams: a) for the RTS network including investments per cases featuring FS-C; and b) for the modified 33-bus network with three grid-connected MGs.

Microgrid	Distribution Node	Distribution Grid	Transmission Node	Microgrid	Distribution Node	Distribution Grid	Transmission Node
MG1	13	DistGrid-1	1	MG13	13	DistGrid-5	8
MG2	18	DistGrid-1	1	MG14	18	DistGrid-5	8
MG3	30	DistGrid-1	1	MG15	30	DistGrid-5	8
MG4	13	DistGrid-2	3	MG16	13	DistGrid-6	13
MG5	18	DistGrid-2	3	MG17	18	DistGrid-6	13
MG6	30	DistGrid-2	3	MG18	30	DistGrid-6	13
MG7	13	DistGrid-3	4	MG19	13	DistGrid-7	15
MG8	18	DistGrid-3	4	MG20	18	DistGrid-7	15
MG9	30	DistGrid-3	4	MG21	30	DistGrid-7	15
MG10	13	DistGrid-4	5	MG22	13	DistGrid-8	19
MG11	18	DistGrid-4	5	MG23	18	DistGrid-8	19
MG12	30	DistGrid-4	5	MG24	30	DistGrid-8	19

Fig. 3. Location of grid-connected MGs and distribution networks.

B. Study Cases

To deal with the research questions stated in Section I, we have defined four test cases corresponding to four different configurations of the overall expansion and operation problem, illustrated in Fig. 4. The results computed for these cases are compared to determine the impact of the choice of the

TSO-DSO coordination model and the provision of local flexibility on the expansion and operation of the system and the associated costs. The provision of local flexibility through FSs is only considered in Case-B and Case-D. These two cases investigate the relationship between the level of the flexibility price and the amount of local flexibility mobilized. In case B, the power exchanges between the TSO and the DSO grids are optimized, i.e., there is efficient coordination of the operation and expansion of the transmission system with the operation of the distribution ones. We call it TSO-DSO coordination. However, in case D, the TSO-DSO power exchanges are determined exclusively according to the decisions made at the distribution and MG levels. Hence, there is no coordination of the expansion and operation of the transmission grid with the operation of the distribution grids (no TSO-DSO coordination). Next, we provide a detailed description of the aim and features of each case and the mathematical formulation of the associated optimization problems.

1) Case A: In this case, no BESs are considered. Therefore, there are no dispatchable DERs and no active MGs connected to the distribution grids. The power exchange on each interface between grids is determined by the net load demand located downstream (including the PV generation). Thus, the power exchange on the border nodes between transmission and distribution, $p^{SS}_{s,t}$, is entered as a parameter in the TEP problem (1) s.t. (2)–(10) to compute the transmission expansion and operation and the associated cost, see Fig. 4.

2) Case B: In this case, the operation of the TSO grid, the DSO grids, and the MGs, together with the expansion of the TSO grid, are jointly optimized and are, therefore, coordinated, considering the provision of local flexibility at the MG level. The OF of the TSO problem is modified to include the cost of flexibility:

$$\min \sum_{ijc\in\mathcal{L}^c} C^{line}_{ijc} ict_{ijc} + \sum_{tg} \Delta t C V_g p_{tg} + \sum_{ti} \Delta t C^{ens} l^{shed}_{ti} + c^{flex}, \tag{79}$$

Within this case, two sub-cases are defined, according to the type of FS provided. There is one where only the provision of FS-C is considered, and there is a second one where only the provision of FS-B is considered. a) In the FS-C case, the flexibility price π^{Cap}_{flex}, and the operation of the whole system and expansion of the TSO grid, are computed by solving the bilevel optimization problem (79) s.t. (2)–(10), (13)–(24), (29)–(52), (60)–(72), and (77)–(78). b) In the FS-B case, the flexibility prices $\pi^{im}_{flex}/\pi^{ex}_{flex}$, and the operation of the whole system and expansion of the TSO grid, are computed by solving (11) s.t. (13)–(21), (25)–(27), (29)–(49), and (53)–(76). Note that the formulation of the above two problems includes the CS conditions of the LL inequality constraints.

3) Case C: In this case, each MG optimizes its energy dispatch without considering the provision of FSs, resulting in a modified MG's OF:

$$\min f^{LL}_m = c^{im}_m - r^{ex}_m, \tag{80}$$

s.t. constraints (29)–(49), not considering the CS conditions.

The solution of each MG's problem yields the profile of the power exchanges with the distribution network ($p^{MG,ex}_{tm} - p^{MG,im}_{tm}$), which are considered as input parameters in the distribution grid's power flow problem that computes the values of $p^{SS}_{ti'}$, $\forall i' \in \mathcal{S}_i$, see Fig. 4. These are then considered as input parameters in the TEP problem, where the transmission expansion and operation are computed along with the associated costs. No coordination of the grids' operation is considered at the DSO-MGs or the TSO-DSOs interfaces.

4) Case D: In this case, the DSO coordinates with the MGs to jointly optimize the provision of local flexibility within the latter in order to reduce the DSO's peak power cost while minimizing the net cost of each MG (see Fig. 4). Two sub-cases are considered within this case. a) In the first one, only the FS-C is mobilized. Then, the flexibility price π^{Cap}_{flex}, and the operation of the DSO grid and MGs, are computed by solving the bilevel optimization problem (11) s.t. (12)–(24) and (29)–(52), (60)–(72), and (77)–(78). In the second sub-case, only the mobilization of the FS-B is considered. b) Then, the flexibility prices $\pi^{im}_{flex}/\pi^{ex}_{flex}$, and the operation of the DSO grid and MGs, are computed by solving (11) s.t. (12)–(21), (25)–(27), (29)–(49), and (53)–(76). The above problem formulations include the CS conditions of the LL inequality constraints. Solving the problems above we compute the values of $p^{SS}_{ti'}$, $\forall i' \in \mathcal{S}_i$, which are entered as input parameters into the TSO, expansion and operation, problem (1) s.t. (2)–(10) solved to compute the investment and operation cost corresponding to the mobilization of the respective FS.

IV. Simulation Results

This section discusses the results computed for the four test cases, which were simulated using the test system described in Section III. As aforementioned, for Case B and Case D, which consider FSs, the simulations were performed considering the mobilization of FS-B and FS-C separately in two different sub-cases. The analysis of the results addresses the research questions stated in Section I. Specifically, the comparison of the investment plan and the system costs for Cases A & B allows us to provide an answer to the second and third research questions, respectively. In addition, the comparison of the MGs' BES dispatch in Cases B, C, & D allows us to answer the first research question.

A. The Role of the TSO-DSO Operation Coordination Model in the Dispatch of Local Flexibility Resources

This section provides a discussion about the management of the MGs' energy resources and how this can be affected by flexibility dispatch. An example of this is given in Fig. 5, which shows the difference in the BES dispatch within MG20 in Case B and in Case D, when it provides FS-C, w.r.t. that in Case C, where no flexibility service is provided (see Fig. 5-c). In Cases B & D, the last discharge half-cycle of the BES of this SG occurs earlier, at a time step within the flexibility activation period, to provide flexibility to the upstream connected systems. The reader should note that the

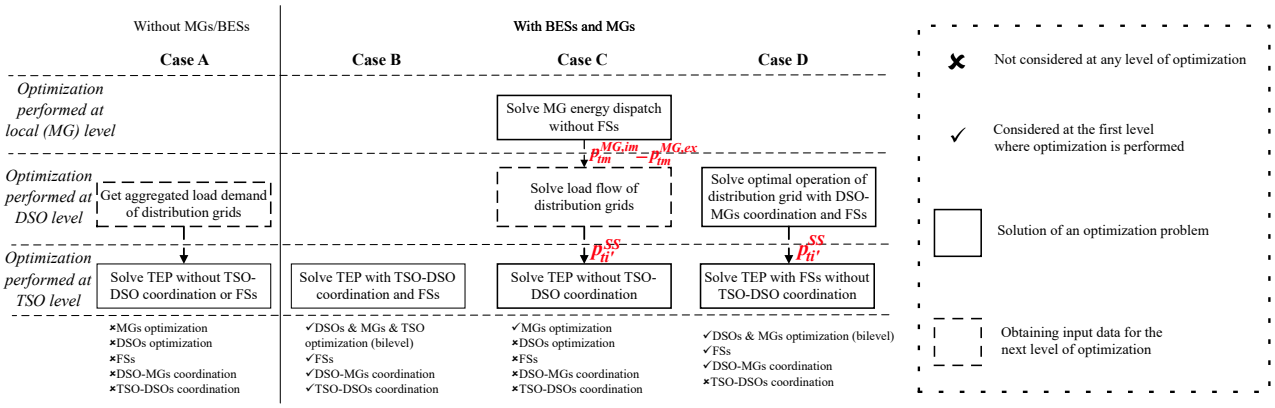

Fig. 4. Case studies considered to investigate the value of local flexibility and its impact on the transmission investments.

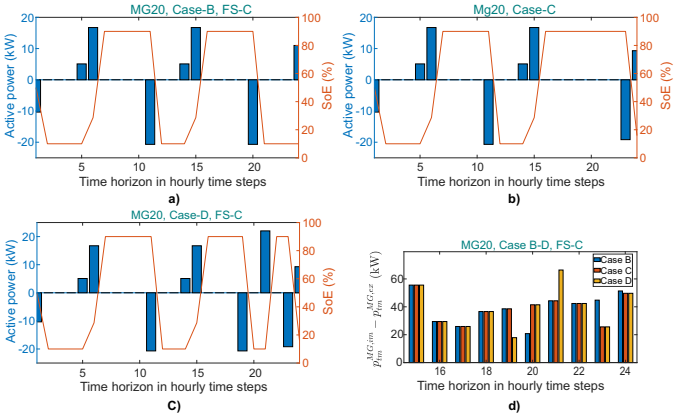

Fig. 5. The BES dispatch of MG20: a) for Case B with FS-C, b) for Case C, c) for Case D with FS-C; and d) the MG's import power in Cases B-D.

flexibility is dispatched at hour 19:00-20:00 in Case B, while it is dispatched at hour 18:00-19:00 in Case D, see Fig. 5-a and Fig. 5-b). This demonstrates that setting up a TSO-DSO coordination scheme can change the output profile of the flexibility resources to satisfy the specific needs of the transmission system. Fig. 5-d shows how the imported power of MG20 is modified in Cases B-D. Right after the flexibility period in Case D, there is large increase in the imported power, as the earlier dispatch of flexibility leaves time for one more BES cycle before the end of the day, which allows the MG to benefit from energy arbitrage. It should be noted, however, that having more frequent cycling of BESs can have a long term cost related to the further degradation of these facilities decreasing their lifetime.

B. The Impact of the Coordination Scheme on the Allocation, Amount, and Value of Local Flexibility

The locations of the MGs that provide FS-C to the TSO in Case B are given in Table I. As can be seen, all the MGs located downstream a transmission bus that requires extra flexibility provide FS-C.

Contrary to the Case B, where the flexibility is procured by the TSO, in Case D all the DSOs make use of the flexibility provided by all the MGs connected to their grids. The amount of flexibility that each MG provides in either Case B or Case D, which is given in Table I, depends only on its location within the distribution grid.

TABLE I
ALLOCATION OF FLEXIBILITY DISPATCH (CASE B, FS-C).

Microgrid	kW	Distribution Node	Transmission Node
MG4	14	13	3
MG5	21	18	
MG6	107	30	
MG19	14	13	15
MG20	21	18	
MG21	107	30	
MG22	14	13	19
MG23	21	18	
MG24	107	30	

Within the case study considered here, the local FSPs did not profit from the provision of FS-B. Similarly, this FS offered no benefit to the DSOs, as in Case D, no flexibility was bought from them, and their operation cost was equal to that of Case C. In Case B, however, the dispatch of the resources within some MGs actually changes with FS-B, even though their cost remains unaltered w.r.t. that in Case C, in order to support the TSO with local flexibility. This indicates that, in Case B, the MGs modify the dispatch of their BESs to provide FS-B at no extra cost or profit for them. Therefore, even though FS-B added no economic value to the daily operation of the MGs or the DSOs, it benefited the investment costs and operation of the transmission system.

The flexibility value of FS-C depends on the choice of P_m^{Cap}, which is affected by the configuration of all connected grids, i.e., it should be customized for each specific test system. In the bilevel formulation, these parameters are eliminated. Therefore, this FS was implemented as the addition of a penalty to the OF of the FSPs and an income from the payment of this penalty to the OF of the TSO in Case B or the DSO in Case D (to understand this, set $P_m^{Cap} = 0$ to (22) and (50)). Moreover, a sensitivity analysis performed about P_m^{Cap} only for Case D showed that when P_m^{Cap} was set to be equal to 25% of the capacity at the MGs' connection points, the DSO and all MGs connected at nodes 13 & 18 had a daily economic value of flexibility of 0.2%, 0.8%, and 1.8%, respectively, of their total daily operation cost. The MGs at nodes 30, however, had an increased cost. Considering that the installed BES capacity at each distribution grid corresponded to a conservative future scenario of BES deployment, it is possible that with the integration of more BESs, this FS-C

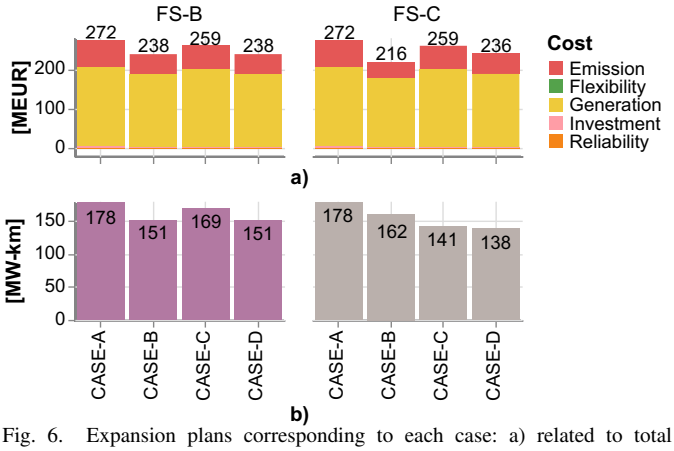

Fig. 6. Expansion plans corresponding to each case: a) related to total expansion cost, and b) related to the total capacity per kilometer deployed.

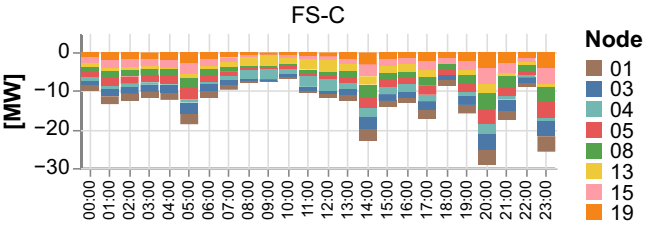

Fig. 7. Comparison of load aggregated and power exchange per node in hourly time steps between Case A and Case B with FS-C, where the net load of Case A is subtracted by the net load of Case B.

could offer an even higher economic value and potentially benefit all connected systems.

C. Impact of the Provision of Local FSs on the TEP

The performance of cases A & B is assessed by comparing the total cost of the operation and expansion of the system corresponding to each case, see Fig. 6. Case A, where no MGs or FSs are considered, yields higher total system costs than any other case, while Case B proves to be the most cost-efficient. A reduction of 12% and 21% in the total system cost, w.r.t. Case A, is achieved in Case B for the mobilization of FS-B and FS-C, respectively. Note that the RTS test system was stressed to encourage investments by increasing the power demand and generation but keeping the transmission capacities. Differences obtained in total system costs are mainly determined by avoiding production using high-cost generation located near the loads and reducing the utilization of congested lines that also changed the power flows. Fig. 7 displays the differences in the aggregated net distribution load, per transmission node and hour of the day, between Case A and Case B, when FS-C is mobilized. The comparison of these two cases shows a notable difference in the net load amount in the transmission nodes 1, 3, 5, and 8, where these differences amount to 1.79 MW, 1.87 MW, 1.88 MW, and 1.85 MW on average, respectively. Interestingly, there are relevant network investments associated with these nodes, affecting lines 1-3, 3-24, 5-10, and 8-9, see Fig. 2-a. The pattern of changes in the net demand due to the provision of local flexibility can be classified into two groups of nodes. In some transmission nodes, like 4 and 13, the net load changes occur in midday hours (10:00-12:00), while in others, like 1, 3, and 5, the changes take place out of the midday hours. These patterns are related to the location of each node and the distribution of power generation. Most of the low-cost generation is located in the northern area (i.e., nodes 11-24) of the transmission grid and its produced energy is shifted through large corridors to the southern area (i.e., nodes 1-10) through lines 21-22 and 9-11.

V. Conclusions

This paper presents an optimization model for the coordination framework of the expansion of the transmission network, the operation of the resources at the transmission and distribution level, and the provision of local FSs. Two types of local FSs are modeled: 1) the baseline FS-B and 2) the capacity limitation FS-C. The FSPs are grid-connected MGs at the distribution system level and their interaction with the upper system levels is formulated as a bilevel optimization problem.

The results computed show that the mobilization of both FSs results in a reduction of the transmission investment cost. Providing FS-C, it was found that the costs faced by the TSO decreased to a larger extent than when FS-B was provided. It was also found, that the transmission costs decreased with the provision of local FSs even in the absence of TSO-DSO coordination, as long as the required local flexibility was procured by the DSOs to support the distribution grid operation. Regarding the economic value of flexibility, it was shown that FS-B only benefited the TSO, while the costs of the DSO and the MGs remained unaffected under this FS. The economic value of FS-C is not straightforward as it is depends the choice of the capacity limit and the configuration of the connected grids and their resources.

The coordination framework presented in this work can be extended to optimize TEP with demand response used by TSOs to consider the demand side in an active role. The model covered the behavior of the final customer with a detailed representation of the FSs and it could easily be used as an analytical and practical tool to evaluate the potential of the value of different local flexibility products in the nearest future. Future studies will consider: 1) scaling the model to simulate large-scale test systems and real-world distribution grids, 2) modeling a more detailed TSO-DSO interface by introducing joint AC OPF for the power flow of both the transmission and the distribution grid, and 3) incorporating a total market environment (i.e., both the spot and local markets) to the TEP for compatibility with the most representative scenarios of the future system operation and applying a comparison between integrated and market-based planning.

Acknowledgement

The work leading to this paper has received fundings from the European Union's Horizon 2020 research and innovation programme for: i) The openENTRANCE project (https://openentrance.eu/) under the grant agreement No. 835896 and ii) The FlexiGrid project (https://flexigrid.org/) under the grant agreement No 864048.

REFERENCES

[1] A. G. Givisiez, K. Petrou, and L. F. Ochoa, "A review on TSO-DSO coordination models and solution techniques," *Elect. Power Syst. Res.*, vol. 189, p. 106659, Dec. 2020.

[2] A. Papavasiliou and I. Mezghani, "Coordination schemes for the integration of transmission and distribution system operations," in *Proc. Power Syst. Computation Conf. (PSCC)*, Dublin, Ireland, 11-15 June 2018.

[3] M. Bolfek and T. Capuder, "An analysis of optimal power flow based formulations regarding DSO-TSO flexibility provision," *Int. J. Electrical Power & Energy Syst.*, vol. 131, p. 106935, Oct. 2021.

[4] M. A. El-Meligy, M. Sharaf, and A. T. Soliman, "A coordinated scheme for transmission and distribution expansion planning: A tri-level approach," *Elect. Power Syst. Res.*, vol. 196, p. 107274, July 2021.

[5] C. Ziras *et al.*, "A mid-term DSO market for capacity limits: How to estimate opportunity costs of aggregators?" *IEEE Trans. Smart Grid*, vol. 11, no. 1, pp. 334–345, Jan. 2020.

[6] M. Pourakbari-Kasmaei, M. Asensio, M. Lehtonen, and J. Contreras, "Trilateral planning model for integrated community energy systems and pv-based prosumers—a bilevel stochastic programming approach," *IEEE Trans. Power Syst.*, vol. 35, no. 1, pp. 346–361, Aug. 2019.

[7] A. A. Bashir, A. Lund, M. Pourakbari-Kasmaei, and M. Lehtonen, "Minimizing wind power curtailment and carbon emissions by power to heat sector coupling—AStackelberg game approach," *IEEE Access*, vol. 8, pp. 211 892–211 911, Nov. 2020.

[8] N. Mohammad and Y. Mishra, "Coordination of wind generation and demand response to minimise operation cost in day-ahead electricity markets using bi-level optimisation framework," *IET Gen., Trans. & Dist.*, vol. 12, no. 16, pp. 3793–3802, Sep. 2018.

[9] J. Von Appen and M. Braun, "Strategic decision making of distribution network operators and investors in residential photovoltaic battery storage systems," *Applied energy*, vol. 230, pp. 540–550, Nov. 2018.

[10] X. Cao, J. Wang, and B. Zeng, "A study on the strong duality of second-order conic relaxation of AC optimal power flow in radial networks," *IEEE Trans.n Power Syst.*, vol. 37, no. 1, pp. 443–455, Jan. 2022.

[11] A. Ramos, E. F. Alvarez, and S. Lumbreras, "OpenTEPES: Open-source transmission and generation expansion planning," *SoftwareX*, in press.

[12] M. Farivar and S. H. Low, "Branch flow model: Relaxations and convexification—-Part I," *IEEE Trans. Power Syst.*, vol. 28, no. 3, pp. 2554–2564, Apr. 2013.

[13] A. J. Gonzalez-Castellanos, D. Pozo, and A. Bischi, "Non-ideal linear operation model for li-ion batteries," *IEEE Trans. Power Syst.*, vol. 35, no. 1, pp. 672–682, Jan. 2020.

[14] C. Barrows *et al.*, "The IEEE reliability test system: A proposed 2019 update," *IEEE Trans. Power Syst.*, vol. 35, no. 1, pp. 119–127, July 2019.

[15] M. E. Baran and F. F. Wu, "Network reconfiguration in distribution systems for loss reduction and load balancing," *IEEE Trans. Power Delivery*, vol. 4, no. 2, pp. 1401–1407, Apr. 1989.

[16] C. A. Sima, M. O. Popescu, C. L. Popescu, and G. Lazaroiu, "Integrating energy storage systems and transmission expansion planning in renewable energy sources power systems," in *Proc. 54th Int. Universities Power Eng. Conf. (UPEC)*, Bucharest, Romania, 3-6 Sep. 2019.

[17] K. Antoniadou-Plytaria *et al.*, "Chalmers campus as a testbed for intelligent grids and local energy systems," in *Proc. 2nd Int. Conf. Smart Grid Energy Syst. & Technol. (SEST) Europe*, Porto, Portugal, 9-11 Ep, 2019.

[18] P. Aristidou and T. Van Cutsem, "A parallel processing approach to dynamic simulations of combined transmission and distribution systems," *In. J. Elect. Power & Energy Syst.*, vol. 72, pp. 58–65, Nov. 2015.

[19] E.ON. E.ON's switch flexibility market. [Online]. Available: https://www.eon.se/foeretag/elnaet/switch/marknader-produkter